13. E. G. Gamalii, S. Yu. Gus'kov, O. N. Krokhin, and V. B. Rozanov, *JETP Lett.* **21**, 70 (1975).

14. H. Azechi *et al.*, *Appl. Phys. Lett.* **49**, 555 (1986).

15. H. Azechi *et al.*, *Phys. Rev. Lett.* **59**, 2635 (1987).

16. R. C. Malone, R. L. McCrory, and R. L. Morse, *Phys. Rev. Lett.* **34**, 721 (1975).

17. LLE Review **31**, 101 (1987).

18. LLE Review **33**, 1 (1987).

19. S. Skupsky, R. W. Short, T. Kessler, R. S. Craxton, S. Letzring, and J. M. Soures, to be published in *J. Appl. Phys.*

20. LLE Review **37**, 29 (1988).

21. LLE Review **37**, 40 (1988).

22. LLE Review **37**, 16 (1988).

23. J. Delettrez, R. Epstein, M. C. Richardson, P. A. Jaanimagi, and B. L. Henke, *Phys. Rev. A* **36**, 3926 (1987).

24. LLE Review **35**, 113 (1988).

1.B The Role of the Rayleigh-Taylor Instability in Burn-Through Experiments

In a previous LLE review article[1] the results of burn-through experiments with barrier layers carried out on the OMEGA laser system were presented and analyzed. In burn-through experiments, the laser irradiates a spherical target that consists of a glass shell or a solid glass sphere overcoated with a parylene layer in which are embedded one or more thin signature layers of moderate-Z material. The onset time of the characteristic x-ray emission lines from a signature layer is then compared to hydrodynamic code simulations. Barrier layers are thin outer coatings that are deposited over the parylene to prevent the early low-intensity laser light from entering the target. While burn-through experiments were originally conceived to study the thermal transport in laser-fusion targets,[2] they are now directed toward the study of the interaction of light with transparent low-Z materials ($Z < 6$). Low-Z ablators are required for advanced target designs in direct-drive inertial-confinement fusion in order to minimize the radiative preheat of the fuel.[3]

The purpose of the experiments described in Ref. 1 had been to study the effect of barrier layers on the burn-through time. The targets were coated with barrier layers of varying material and thickness: Al, KCl, CsI, and two thicknesses (0.015 μm and 0.05 μm) of Au, and

illuminated by the 24 beams of the OMEGA laser system at 0.351 μm. The simulations were carried out with the one-dimensional hydrodynamic code *LILAC* at nominal intensity (I_0, defined as the laser peak power divided by the initial target radius), and at increasing laser intensities until the simulation burn-through time agreed with the experimental value. The target conditions and the experimental and simulation results are summarized in Table 40.I. The experimental results show that the burn-through times increase with the nuclear Z of the barrier material (except for the KCl case) and that there is a large difference in burn-through time between the bare-parylene target and the aluminum-coated target. In contrast, the simulation results indicate that there is little difference among the burn-through times for all the barrier layers, except for the 0.05-μm gold case, and that the addition of these barrier layers changes the burn-through time by at most 50 ps. The burn-through time itself is not the best quantity for analyzing the results because comparison can only be made between cases with the same target conditions (especially the parylene thickness) and laser parameters (laser intensity and pulse width). A preferable quantity is the laser intensity (I_m) required in the simulations to match the measured burn-through times. In the case of the no-barrier-layer target, large burn-through rates were measured: Laser intensities over ten times nominal are required in simulations to obtain the observed burn-through time. For the Al-barrier-layer target, laser intensities of only three times nominal reproduced the experimental value. For the thick-gold target, only one and a half times nominal intensity is needed to match the observed burn-through times. The KCl case is an exception to the trend: KCl seems to behave partly like parylene and partly like an opaque conductor.

In order to attempt to explain these results, the possibility that the following processes could lead to enhanced burn-through rate was investigated with *LILAC*:

Table 40.I: Onset times of the x-ray emission from the signature layer for the various barrier-layer targets. Tabulated are the measured burn-through times and the simulation burn-through times for increasing laser intensity. All times are with respect to the peak of the pulse. The last column indicates the intensity I_m required in simulations to match the measured burn-through times.

Barrier Layer	Z	Laser Intensity (W/cm^2)	Burn-Through Times (ps)						I_m/I_o
			Measured	Simulation					
				1.5 I_o	2 I_o	3 I_o	5 I_o	10 I_o	
none	–	8.1×10^{14}	-250 ± 20	~400	150	20	-100	-220	12.3 ± 1.3
0.1-μm Al	13	7.5×10^{14}	-25 ± 20	nb	~350(120)	70	-50	-170	4.1 ± 0.4
0.1-μm KCl	18	8.2×10^{14}	-150 ± 20	290	140	30	-80	-180	7.4 ± 0.6
0.1-μm CsI	54	8.0×10^{14}	0 ± 20	~400	160	40	-60	-160	4.1 ± 0.2
0.015-μm Au	79	7.9×10^{14}	125 ± 20	270	140	30	-60	-130	2.1 ± 0.2
0.05-μm Au	79	7.9×10^{14}	350 ± 20	320	210	160	-100	–	1.5

Time in parentheses is for the Al case run with the KCl laser conditions.

TC 2608

−hot-spot intensities exceeding ten times nominal;

−shine-through of the laser light early in the pulse (or a prepulse) while the parylene layer is still transparent;

−a prepulse that would ablate part of the bare-parylene layer; and

−self-focusing of the hot spots and filamentation.

From a detailed analysis[1] of these processes it was concluded that none could explain the experimental results. A brief summary of the reasons is presented here. Hot-spot intensities of ten times nominal in the laser-illumination distribution on target would require hot spots about 40 times nominal in the single-beam distribution because the superposition of the 24 beams of OMEGA smooths out the illumination pattern (at least four beams overlap at any point on the target surface). Yet, both x-ray imaging and equivalent-target-plane imaging do not show the presence of hot spots with such large intensities. Also, the barrier layers are not expected to smooth out the hot spots. Prepulse measurements on the OMEGA laser have led to the conclusion that, if a prepulse existed, its energy would be less than 1 mJ. Such a prepulse cannot ablate enough material to account for the large differences in the burn-through times. As for filamentation and self-focusing, the growth lengths for filamentations are much larger than the electron-density scale lengths prior to the burn-through times. While the growth lengths for ponderomotive self-focusing of hot spots are of the same order as the electron-density scale lengths, it is not expected that barrier layers should affect self-focusing because the growth lengths are independent of Z.

While shine-through alone does not affect the burn-through rate, it can lead to conditions that can enhance the growth of the Rayleigh-Taylor instability, which occurs when a light fluid is accelerated against a heavier fluid and could cause the large, observed burn-through rates by mixing signature-layer material into the parylene layer. Because of its importance, the process will be described in detail and illustrated in Fig. 40.5, where the density and temperature profiles are shown at times of interest. The initial conditions at room temperature are given in Fig. 40.5(a) where the laser comes from the right. Shine-through assumes that, because parylene is transparent to UV light at room temperature,[4] laser light penetrates to the signature layer early in the pulse before breakdown occurs. This process is very attractive because it would explain both the effect of adding a thin barrier layer of aluminum and the difference in burn-through times between the Al and KCl cases. (CsI is also transparent at room temperature, but its use as a photocathode material implies that free electrons can be created very quickly by the laser pulse.) The aluminum layer is thick enough to block most of the laser light early in the pulse (0.1 μm of aluminum has an optical density of about 3.0 for 350-nm light), while KCl seems to behave partly like parylene and partly like an opaque conductor. An opaque barrier layer can prevent prepulses or the early part of the pulse from penetrating into the target and depositing energy inside the target after breakdown has occurred. Breakdown thresholds from high-intensity laser illumination in

parylene and glass are not well known.[5] In the targets used in this experiment, breakdown probably occurs at the parylene-signature-layer interface, especially when the signature layer is an opaque material that absorbs some of the laser light reaching it. This interface can also be the site for impurity deposition during the target-coating process and for target imperfections.[6]

Shine-through was studied using *LILAC* by assuming that, very early in the pulse, the parylene is transparent and absorbs a small fraction of the laser light. At a given intensity threshold, estimated to be about 1×10^{12} W/cm^2 in single-beam shine-through experiments,[4] the breakdown at the interface is modeled by depositing the laser light at the boundary of the parylene and signature layers. The electron temperature increases in the region immediately in front of the deposition region because of thermal conduction. As the parylene ionizes or breaks down, a critical surface is created in that region. Figure 40.5(b) shows conditions in the parylene immediately after the breakdown was initiated. Because it is difficult to model the ionization of parylene at solid density and temperatures below 10 eV, this critical surface cannot be created self-consistently. Instead, the laser light is deposited in the zone where the electron temperature reaches 5 eV (varying this threshold temperature made little difference). This causes an "ionization wave" to propagate quickly from the signature layer toward the target surface [see Fig. 40.5(c)]. At that point, the parylene layer is a slowly expanding plasma with temperatures of a few electron volts and density varying between one-third solid and almost three times solid density. As the laser intensity increases in time, the critical surface reaches the outer surface of the target at about 920 ps before the peak of the pulse [Fig. 40.5(d)]. An ablation surface is established [Fig. 40.5(e)] and the parylene is recompressed. In Fig. 40.5(f), the glass shell is now being compressed by the ablation process. The low-density cavity in the parylene, at the glass-parylene interface, persists until the parylene is completely ablated away. For comparison, the usual development of the ablation front in the absence of shine-through is illustrated in Fig. 40.6. In this case the low-density cavity is much more shallow, and the ratio of the density at the outer glass surface to that of the inner parylene surface is much smaller than for the shine-through case. The one-dimensional burn-through times are not affected much by shine-through because the evolution of the heat front in the initial Lagrangian frame of the materials is not much different in the two cases. However, the nonuniform energy deposition at the parylene-signature-layer interface may lead to a nonuniform low-density plasma in the parylene layer by the time the ablation surface is established. These conditions may seed the Rayleigh-Taylor instability during the implosion, which may lead to a mixing of signature-layer material into the parylene.

We now consider the Rayleigh-Taylor instability in greater detail. The instability can occur in two regions of the target: at the ablation surface and at the parylene-signature-layer interface. Near the ablation surface, the cold, dense shell material is accelerated by the hot, less-dense ablating material during the inward acceleration phase of the
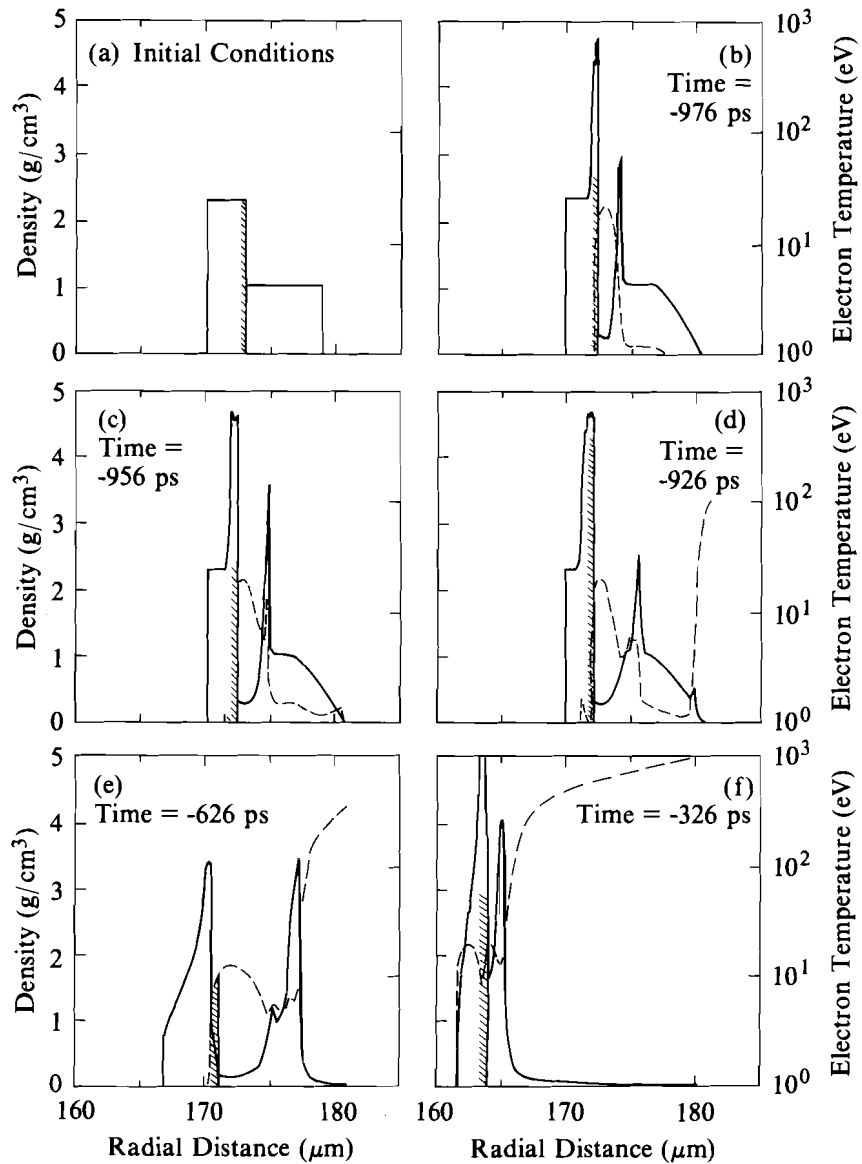
TC2611

Fig. 40.5
Evolution of the density (solid line) and temperature (dashed line) profiles under shine-through conditions. The target consists of a 3-μm glass shell overcoated with 6 μm of parylene. (a) Initial conditions; the laser comes from the right; (b) 50 ps after the breakdown at the interface; (c) the ionization wave is moving toward the outer surface; (d) the critical surface is established at the outer surface; (e) the parylene is being recompressed by the ablation process; (f) the glass shell is now compressed and is accelerated inward. The low-density cavity in the parylene persists until the parylene is ablated away.

pellet implosion. This situation is analogous to the classical Rayleigh-Taylor fluid instability[7] and is often referred to as the acceleration phase or ablation-surface instability. Numerical simulations have shown, however, that the linear and nonlinear growth rates for the ablation-surface instability are different from those expected from the classical case because they are modified by the ablation process.[8,9] In the burn-through experiments the possible existence of unstable flow development is further complicated by the presence of the unstable interface located at the CH_x-signature-layer boundary, where the lighter parylene is accelerated against the denser signature-layer material. The evolution of this interface is expected to be nearly classical with an Atwood number less than 1. The Atwood number is defined as $[(\rho_H - \rho_L) / (\rho_H + \rho_L)]$, where ρ_H is the density of the heavy fluid (the signature-layer material) and ρ_L is the density of the light fluid (parylene).

The Rayleigh-Taylor instability is analyzed by decomposing the fluid perturbation into Legendre modes. The evolution of the instability is then characterized by the growth rates of these modes. In the references cited above, the growth rates were calculated mostly for single modes. Recently, a number of experimental and theoretical studies[10,11] have shown that the contributions of all potentially unstable modes and their mode-mode interactions must be considered. The treatment of all of these modes, including both their linear and nonlinear evolutions, during the pellet implosion is presently beyond the capabilities of ICF simulation codes. However, models have been developed[11] that estimate the unstable growth and the potential effect of the Rayleigh-Taylor instability on pellet implosions from the zeroth-order (unperturbed) hydrodynamic information obtained from one-dimensional simulations. The evolution of the unstable growth is carried out on a noninterfering basis, i.e., the effect of the instability is not fed back into the one-dimensional simulation.

A model similar to that described in Ref. 11 has been developed to estimate the amount of shell distortion and mixing that could take place during the implosion of burn-through targets. This model computes the modal amplitudes due to the Rayleigh-Taylor unstable flow development and estimates from these amplitudes the mixing region depth $\epsilon\sigma_{rms}$[11] as a function of time, where ϵ has value of order unity and σ_{rms} is given by

$$\sigma_{rms} = \left[\frac{1}{4\pi} \sum_{l>1} \sum_{m} |A_{lm}|^2 \right]^{1/2} ,$$

where A_{lm} are modal coefficients and the sum is over modes 1 to 200. Linear growth rates for low-Z ablators, which have short density scale lengths, can be expressed as $\gamma = \alpha\sqrt{ka} - \beta k V_a$, where k is the unstable mode wave number; a, the acceleration; and V_a, the ablation velocity given by $\dot{m}/\hat{\rho}$ ($\dot{m}$ is the mass flux rate and $\hat{\rho}$, the peak density).[8,12] The constant values $\alpha \approx 0.90$ and $\beta \approx 3\text{-}4$ provide an adequate fit to the growth rates obtained from full two-dimensional
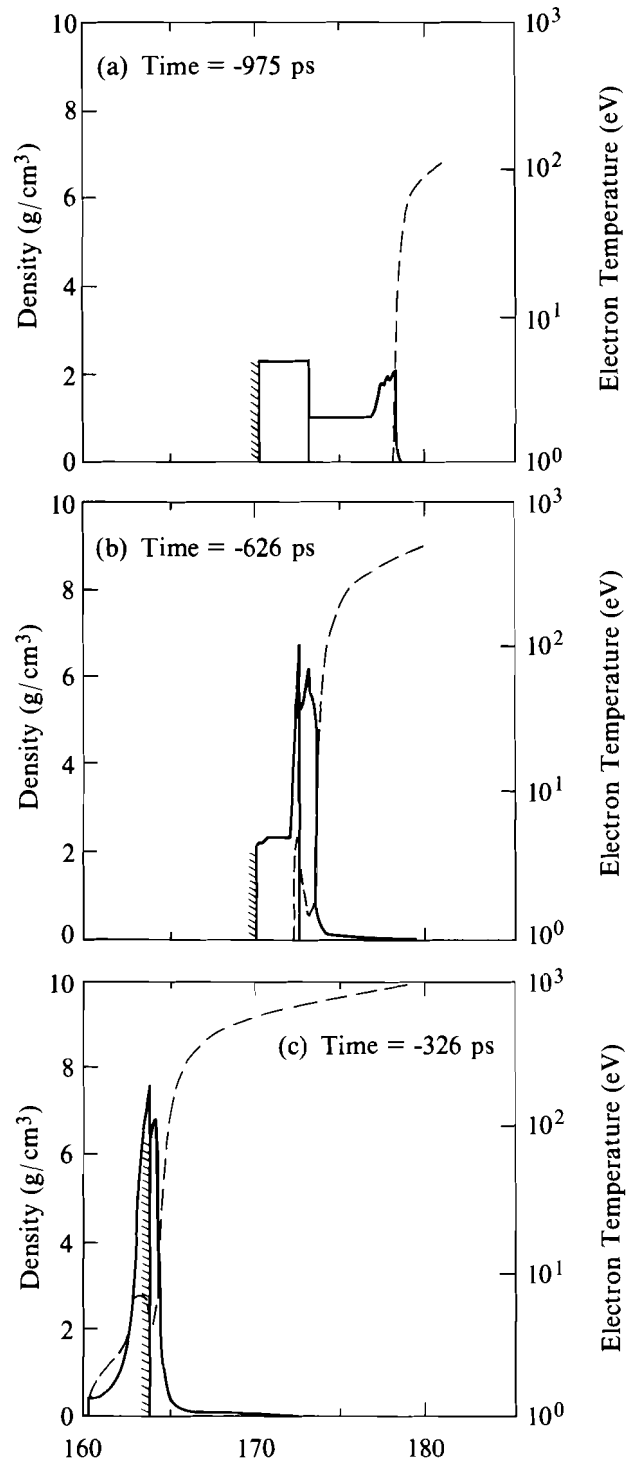
Fig. 40.6
Evolution of the density (solid line) and temperature (dashed line) profiles under the usual simulation conditions. The target is the same as in Fig. 40.5. (a) Laser energy is deposited at the outer surface and the shock wave is compressing the parylene; (b) the shock wave is entering the glass shell; (c) the shell is accelerated inward. The cavity at the interface is shallower than in Fig. 40.5.

TC2612

simulations over a wide range of initial parameters. Comparisons with growth rates determined by two-dimensional simulations with *ORCHID*[13] for the experiments of interest showed that this expression with $\beta = 3$ gives a reasonable fit. The model tracks the growth of individual modes using the linear growth rates until some saturation amplitude is reached. As the instability evolves, bubbles develop toward the high-density side of the ablation surface and spikes grow toward the outside of the target. In the case of the ablation surface instability, we are interested in the development of the bubble, which has the potential of reaching into the signature layer. After a given mode has reached the nonlinear regime, the amplitude of the bubble (mode) is assumed to continue to grow linearly in time.[14] (Studies have shown that, for finite fluid layers and during the nonlinear evolution, the motion of the bubble departs from constant velocity as the layer thickness gets smaller.[15] However, since this model is used only to illustrate the potential effects of the instability, no attempt has been made to treat the nonlinear stage more accurately.)

The model also calculates the evolution of the parylene-signature-layer interface instability during the implosion. The linear growth rates used for the interface instability are given by $\gamma = \sqrt{Aka \ / \ (kL + 1)}$, where L is the mass-density scale length. In this case we want to estimate to what extent the signature-layer material can penetrate into the parylene layer. We have adopted the spike amplitude suggested in Ref. 11 to estimate the extent of the spike penetration into the ablation region.

In order to obtain an estimate of the mixing-layer depth in burn-through targets, we consider a range of simple initial-amplitude cases. We assume that the laser illumination nonuniformity produces the dominant source of initial-amplitude seeds to the Rayleigh-Taylor instability, which can be represented by $\xi = \xi_0 \exp[-(\Delta R/R)\ell]$ (μm/mode), where ΔR is the separation distance between the ablation and critical surfaces; R, the target radius; and ℓ, the Legendre mode number.[16] For the first case we consider $\Delta R/R = 0.05$ and three values of ξ_0 such that $\sigma_{rms1} = 0.304$ μm, $\sigma_{rms2} = 0.167$ μm, and $\sigma_{rms3} = 0.0304$ μm. For the second case we set $\Delta R/R = 0.01$ and adjust ξ_0 such that the same values of σ_{rms} are obtained. The targets are 3-μm glass shells coated with parylene thicknesses varying from 4 μm to 10 μm and with radii and incident laser intensities similar to those in the experiments described in this article. The simulations were run in the usual absorption mode, without shine-through effects. Figure 40.7 displays an example of the model prediction for the thickness of the mix layers that could potentially be generated by the growth of the Rayleigh-Taylor instability as a function of time for two cases: a 4-μm parylene layer [Fig. 40.7(a)] and a 6-μm parylene layer [Fig. 40.7(b)]. The initial conditions for both cases are $\sigma_{rms} = 0.167$ μm and $\Delta R/R = 0.05$ μm. The solid line is the in-flight thickness of the overdense parylene, defined as the difference between the position of the overdense portion of the target and the position of the parylene-glass interface. The position of the overdense portion of the target is determined by searching for the location of the peak in the density from the outer radius inward and determining the radial location of the

e-fold from the peak density outward. The dashed lines show the increase with time of the thicknesses of the unstable regions associated with the ablation-surface (A) and with the parylene-glass interface (I). For the initial conditions used in this example, the ablation-surface instability has the largest mixing region. No interfacial coupling was assumed between the ablation surface and the parylene-glass interface in order to illustrate the respective evolution of the two unstable regions. If a coupling of the form $\exp(-k \, \Delta R)$,[7] where ΔR is the distance between the two surfaces, was assumed, larger growth would be obtained at the parylene-glass interface.

The signature times, defined as the time of the earliest crossover of either of the dashed curves with the parylene thickness curve, are shown in Fig. 40.8 for parylene thicknesses of 4 to 10 μm. The curves labeled 1, 2, and 3 represent the signature times for the cases with initial amplitude of 0.304 μm, 0.167 μm, and 0.0304 μm, respectively. Figure 40.8(a) is for $\Delta R/R = 0.05$ and Fig. 40.8(b), for $\Delta R/R = 0.01$. The resulting signature times show that, depending on the modal spectrum and amplitudes, the Rayleigh-Taylor instability could grow fast enough to cause the signature-layer material to reach the heat front and emit at the early times observed in the experiments. For example, curve 2 for $\sigma_{rms} = 0.167$ μm in Fig. 40.8(a) yields signature times close to the observed burn-through time for the bare parylene target (-250 ps). The signature times from the mixing model should be used only as an indication because they were obtained with a simplified model of the evolution of the Rayleigh-Taylor instability and were based on a reasonable guess of the amplitude and spectrum of the initial perturbations. The results do indicate, however, that for reasonable rms-perturbation levels, the Rayleigh-Taylor instability could potentially lead to the early mixing of low-Z ablator and signature materials.

The effect of adding different types of barrier layers on the signature times obtained from the mixing model could be explained as follows. Early shine-through can create density perturbations at the parylene-signature-layer interface as was discussed previously and these perturbations can seed the Rayleigh-Taylor instability. The addition of an opaque barrier layer would reduce the amount of shine-through light reaching the interface, thus reducing the initial perturbations and delaying the signature times as shown in Fig. 40.8. For example, while in Fig. 40.8(a) an initial amplitude with $\sigma_{rms} = 0.167$ μm (curve 2) is needed to match the observed burn-through time for the bare-parylene target, the smaller value of 0.0304 μm (curve 3) is required to match the burn-through time of the Al-barrier-layer target. The lower value of initial amplitude could explain the difference in burn-through times between the bare-parylene case and the aluminum-barrier-layer case. As to the effect of adding different types of barrier layers, the various layers would let different amounts of laser light shine through, producing variations in the initial perturbation. For example, KCl is probably more transparent to the laser light than aluminum; thus, the KCl-coated targets would sustain larger initial perturbations than the aluminum-coated target. Also the difference in the burn-through time between the thick-gold case and the thin-gold
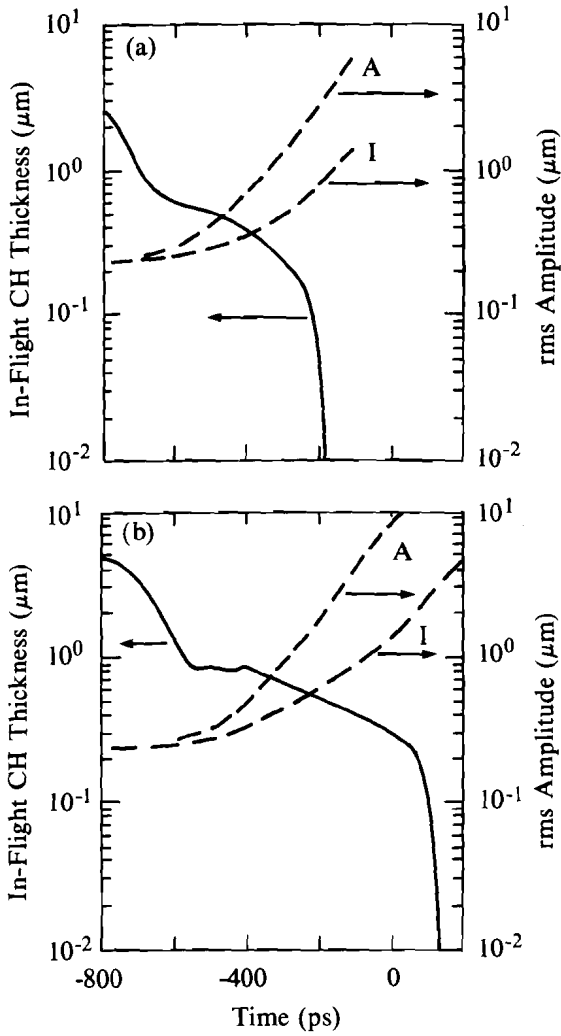
TC2606
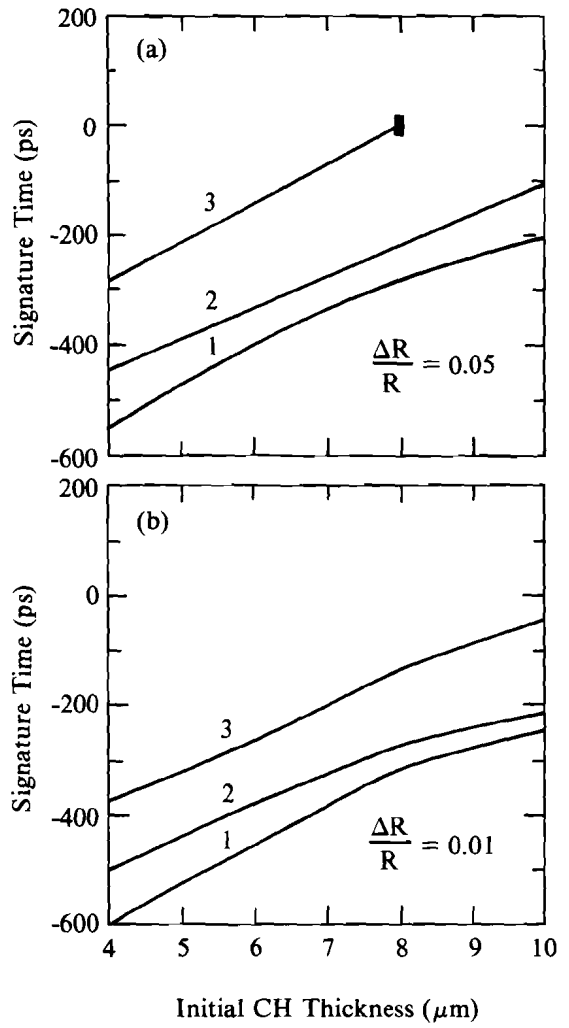
TC2607

Fig. 40.7
Results of the Rayleigh-Taylor instability mixing model for a glass shell coated with (a) 4 μm of parylene and (b) 6 μm of parylene. The solid line is the temporal evolution of the parylene thickness and the dashed lines the evolution of the thickness of the unstable (mixing) region for the ablation-surface instability (A) and the glass-parylene-interface instability (I). The initial perturbation has a $\sigma_{rms} = 0.167$ μm and $\Delta R/R = 0.05$ in both cases. The earliest crossing of one of the solid lines with the dashed lines is taken as the onset time of emission from the glass shell due to mixing.

Fig. 40.8
Onset time of emission from the glass shell obtained from the mixing model as a function of the parylene thickness for $\Delta R/R$ = 0.05 (a) and 0.01 (b). Curves 1, 2, and 3 are for initial perturbations with σ_{rms} = 0.304 μm, 0.167 μm, and 0.0341 μm, respectively. The solid rectangle at the end of curve 3 for $\Delta R/R$ = 0.05 indicates the signature layer does not mix through the parylene layer for larger thicknesses.

case, which can be partially explained by the *LILAC* simulations from the increase in the amount of gold to be heated and ablated (about 60 ps out of the 225-ps difference), could be due to differences in the early shine-through (the thick-gold layer is more opaque than the thin-gold layer) and by increased radiation preheat from the thick-gold barrier layer, which radiates for a longer time than the thin one. Radiation preheat tends to increase the density gradients in the target, thus reducing the Rayleigh-Taylor growth rate.

The preceding analysis of mixing due to the Rayleigh-Taylor instability may explain the fast burn-through rates observed in the experiment. However, it should be noted that, if the Rayleigh-Taylor instability was present, its effects on the implosion dynamics might not be observable experimentally. *LILAC* simulations of OMEGA gas-filled and cryogenic target implosions[17] show reasonable agreement with experimental observables, such as laser energy absorption, x-ray conversion for moderate-Z materials, implosion velocity, and time of core formation. This indicates that the unperturbed one-dimensional flow obtained by *LILAC* approximates well the gross features of the implosions. Numerical simulations of the development of the nonlinear evolution of Rayleigh-Taylor unstable flow have shown that there exists no large departure in the motion of the centroid of mass of the shell between implosions that are uniform and those that are distorted due to unstable growth.[13] Therefore, if the Rayleigh-Taylor instability was present in the burn-through experiment, it might not be possible to confirm its presence with the usual array of diagnostics deployed during OMEGA experiments.

Summary

We had previously reported on burn-through experiments with barrier layers consisting of different materials and thicknesses that showed burn-through occurring progressively later during the pulse for the following succession of barrier layers: none, aluminum, thin gold, and thick gold. Simulation results had predicted that there should be only small differences (~ 50 ps) among the burn-through times of all the barrier layers, except for the thick-gold barrier layer. None of the following processes could adequately explain the experimental results: severe hot spots (intensities ten times nominal), shine-through, the presence of a prepulse, filamentation, and self-focusing. We now have shown that the Rayleigh-Taylor instability has the potential of mixing signature-layer material far enough into the parylene that early-time x-ray emission from the signature layer would be observed. The effect of an opaque barrier layer would be to prevent the target damage caused by shine-through, thus reducing the initial perturbations that seed the instability. Varying the material and the thickness of the barrier layer would affect the shine-through, which would vary the seed of the instability. Since little is known about the transmission and breakdown characteristics of materials to 350-nm laser light at laser intensities below 10^{13} W/cm^2, experiments are planned to understand the shine-through behavior of thin barrier layers. Finally, burn-through-type experiments with improved laser-illumination uniformity could provide qualitative information on the degree of mixing of the signature layer into parylene due to the Rayleigh-Taylor instability.

ACKNOWLEDGMENT

REFERENCES

1. LLE Review **35**, 113 (1988).

2. J. Delettrez, *Can. J. Phys.* **64**, 932 (1986); P. A. Jaanimagi, J. Delettrez, B. L. Henke, and M. C. Richardson, *Phys. Rev. A* **34**, 1322 (1986).

3. LLE Review **23**, 125 (1985).

4. T. Boehly, D. Bradley, and J. Delettrez, paper H6, 19th Annual Anomalous Absorption Conference, Durango, CO (1989).

5. N. Bloembergen, *IEEE J. Quantum Electron.* **QE-10**, 375 (1974); LLE Review **35**, 125 (1988); W. Seka (private communication).

6. H. Kim (private communication).

7. G. Taylor, *Proc. R. Soc. London, Ser. A:* **201**, 192 (1950); D. J. Lewis, *Proc. R. Soc. London, Ser. A:* **202**, 81 (1950); S. Chandrasekhar, *Hydrodynamic and Hydromagnetic Stability*, (Clarendon Press, Oxford, England, 1961), Chap. 10.

8. H. Takabe, K. Mima, L. Montierth, and R. L. Morse, *Phys. Fluids* **28**, 3676 (1985).

9. M. H. Emery, J. H. Gardner, and J. P. Boris, *Phys. Rev. Lett.* **48**, 677 (1982); C. P. Verdon, R. L. McCrory, R. L. Morse, G. R. Baker, D. I. Meiron, and S. A. Orszag, *Phys. Fluids* **25**, 1653 (1982).

10. K. I. Read, *Physica 12d*, 45 (1984); D. L. Youngs, *Physica 12d*, 32 (1984).

11. S. W. Haan, *Phys. Rev. A* **39**, 5812 (1989).

12. S. E. Bodner (private communication); M. Tabak (private communication).

13. *ORCHID* is a two-dimensional Lagrangian hydrodynamic code that is described in some length in Ref. 3.

14. G. Birkhoff and D. Carter, *J. Math. Mech.* **6**, 769 (1957); P. R. Garabedian, *Proc. R. Soc. London, Ser. A:* **241**, 423 (1957).

15. G. R. Baker, D. I. Meiron, and S. A. Orszag, *Phys. Fluids* **23**, 1485 (1980).

16. S. E. Bodner, *J. Fusion Energy* **1**, 221 (1981).

17. R. L. McCrory, J. M. Soures, C. P. Verdon, F. J. Marshall, S. A. Letzring, S. Skupsky, T. J. Kessler, R. L. Kremens, J. P. Knauer, H. Kim, J. Delettrez, R. L. Keck, and D. K. Bradley, *Nature* **335**, 225 (1988).